IEEE Access
Multidisciplinary ⋮ Rapid Review ⋮ Open Access Journal

Received October 20, 2020, accepted November 9, 2020, date of publication November 11, 2020,
date of current version November 27, 2020.

Digital Object Identifier 10.1109/ACCESS.2020.3037522

Highly Sensitive Temperature Sensor Based on All-Fiber Polarization Interference Filter With Vernier Effect

BO HUANG[1,2], YING WANG[1,2], CHANGRUI LIAO[1,2], (Member, IEEE), AND YIPING WANG[1,2,3], (Senior Member, IEEE)

[1]Key Laboratory of Optoelectronic Devices and Systems, Ministry of Education and Guangdong Province, College of Physics and Optoelectronic Engineering, Shenzhen University, Shenzhen 518060, China
[2]Guangdong and Hong Kong Joint Research Centre for Optical Fibre Sensors, Shenzhen University, Shenzhen 518060, China
[3]Shenzhen Photonic Sensing Technology Co., Ltd., Shenzhen 518172, China

Corresponding author: Ying Wang (yingwang@szu.edu.cn)

This work was supported in part by the National Natural Science Foundation of China (NSFC) under Grant 61675137 and Grant 61905166, in part by the China Postdoctoral Science Foundation under Grant 2019M653021 and Grant 2018M643162, in part by the Science and Technology Innovation Commission of Shenzhen under Grant JCYJ20170818093743767, and in part by the Development and Reform Commission of Shenzhen Municipality Foundation.

ABSTRACT A novel highly sensitive temperature sensor based on all-fiber polarization interference filter with Vernier effect is proposed and experimentally demonstrated in this article. The all-fiber polarization interference filter, namely Lyot filter, is simply consisted of a section of polarization-maintaining fiber positioned between two linear fiber polarizers. Vernier effect is introduced by simply cascading a Fabry–Perot interference with the Lyot filter. The temperature characteristics of the Lyot filter without and with Vernier effect are experimentally investigated, respectively. The experimental results show that with Vernier effect, the temperature sensitivity of Lyot filter can be improved from −1.752 nm/°C to −25.289 nm/°C. To the best of our knowledge, this is the first demonstration of Lyot filter based temperature sensor combining with Vernier effect. The good performance of the Lyot filter with Vernier effect in temperature sensing not only provides a new option for the optical fiber temperature sensor, but also further broadens the application of Lyot filter in the sensing field.

INDEX TERMS Optical fiber sensors, temperature sensor, fiber birefringence, polarization interference, fiber filters.

I. INTRODUCTION

In the past few decades, with the rapid development of the emerging industries including the Internet of Things, artificial intelligence, autonomous driving and so on, the sensor industry has also ushered in new development opportunities. Among the numerous kinds of sensors, optical fiber sensor has attracted a lot of research interest due to its unique advantages such as simple structure, light weight, immunity to electromagnetic interference, etc. So far, a variety of optical fiber sensors with different techniques have been developed by researchers and successfully achieved the measurement of different parameters such as torsion [1], [2], transverse load [3], temperature [4], gas pressure [5] and so on. Among the various parameters, temperature is an important physical parameter in all fields of natural science, industrial manufacture as well as most aspects of daily life. And accordingly, great efforts have been made to develop the optical fiber temperature sensor.

Currently, the development of optical fiber temperature sensors are mainly based on two technical routes: fiber grating based temperature sensors [6]–[14] and fiber interferometer based temperature sensors [15]–[28]. For fiber grating based temperature sensors, long period grating (LPG) is a common employed device [6]–[10]. Bhatia *et al.* have proposed a bare LPG based temperature sensor [6]. Ye *et al.* have demonstrated a temperature sensor based on a LPG written in commercially available boron-doped fibers [7]. Rao *et al.* have reported a special photosensitive single mode fiber based LPG for temperature sensing [8]. And

The associate editor coordinating the review of this manuscript and approving it for publication was Muguang Wang.

then, Zhang *et al.* have presented a sandwiched LPG to measure temperature [9]. Wang *et al.* have developed a CO_2-laser-notched LPG based temperature sensor [10].

However, owning to the inherent characteristics of LPG, LPG based temperature sensors are also sensitive to the refractive index, bend, transverse load and so on, which is a barrier to the practical application. Meanwhile, Fiber Bragg Grating (FBG) based temperature sensors have attracted great attention for their stability in the practical application [11]–[14]. Grobnic *et al.* have firstly reported a sapphire FBG sensor made by femtosecond laser radiation for ultrahigh temperature sensing [11]. Zhang *et al.* have designed a novel hydrogen-loaded germanium-doped FBG based high-temperature resistance temperature sensor [12]. Sengupta *et al.* have employed a superstructure FBG to fulfill temperature sensing [13]. In addition, Sridhar *et al.* have proposed a multi-layer MoS_2 coated etched FBG based temperature sensor [14]. And yet, the highest sensitivity of the above mentioned FBG based temperature sensors is only ∼0.095 nm/°C, which is relatively low and has yet to be further improved. Compared to fiber grating based temperature sensors, fiber interferometer based temperature sensors are much more desirable sensors and have gradually become the most widely used optical fiber temperature sensors for their simple structure and high sensitivity. The fiber interferometers employed to construct temperature sensors mainly contain Fabry–Perot interference (FPI) [15]–[18], Michelson interferometer (MI) [19], [20], Mach–Zehnder interferometer (MZI) [21]–[23] and Sagnac interferometer (SI) [24]–[30], which are fabricated by using different kinds of fibers including thin core fiber [15], single mode fiber [19]–[22], microfiber [23], [30], polarization maintain fiber [24]–[26], [28], photonic crystal fiber [27], [29] and so on. Among the above mentioned fiber interferometers, a very high temperature sensitivity of −16.38 nm/°C has been achieved with an isopropanol cladding elliptical microfiber based SI [30]. However, the fabrication of the isopropanol cladding elliptical microfiber is a complicated process that involves femtosecond laser micromachining, fiber taper drawing and encapsulation, which is a large obstacle for practical application.

Lyot filter, as a type of polarization interference filter firstly developed in 1933 [31], has been widely employed in the visible and near infrared. In the traditional Lyot filter design, it is consisted by positioning a birefringent element between a single pair of polarizers. After 80 years of development, Lyot filter has evolved from bulk Lyot filter [32]–[34] to bulk-fiber mixed Lyot filter [35], [36] and further to all fiber Lyot filter [37]–[41]. While its size is more and more compact, the application area of Lyot filter has been confined to spectral imaging [33], [34], laser [35], [36], and communication [37], [38]. Until recently, with the advent of all fiber Lyot filter, Lyot filter based fiber sensor has been achieved and then worked as torsion sensor [39]–[41], transverse load sensor [41] and gas pressure sensor [5], respectively. And yet, the application of Lyot filter in the field of temperature sensing is rarely reported. In this article, a novel highly sensitive temperature sensor based on all-fiber polarization interference filter with Vernier effect is proposed and experimentally demonstrated. The all-fiber polarization interference filter, namely Lyot filter, is simply consist of a section of polarization-maintaining fiber (PMF) positioned between two linear fiber polarizers. The temperature characteristic of Lyot filter is firstly analyzed and experimentally investigated. The obtained experimental results indicate that the employed Lyot filter can achieve temperature sensing with a sensitivity of −1.752 nm/°C, confirming the feasibility of Lyot filter based temperature sensor. And then, Vernier effect is introduced into the Lyot filter based temperature sensor by simply cascading a FPI. By tracking the wavelength shift of the envelope, the temperature measurement can be achieved with an extremely high temperature sensitivity up to −25.289 nm/°C. To the best of our knowledge, this is the first demonstration of Lyot filter based temperature sensor combining with Vernier effect. By simply cascading a HCF based FPI, the combination of Lyot filter and the Vernier effect can be easily achieved and significantly improves the temperature sensitivity of Lyot filter from −1.752 nm/°C to −25.289 nm/°C, which is no costly and complicated treatment process required. The good performance of the Lyot filter with Vernier effect in temperature sensing not only provides a new option for the optical fiber temperature sensor, but also further broadens the application of Lyot filter in the sensing field.

II. PRINCIPLES AND TEMPERATURE CHARACTERISTIC OF LYOT FILTER

Figure 1 is the schematic diagram of the proposed all-fiber Lyot filter, which is comprised of a section of PMF and a single pair of fiber polarizers. In the all-fiber Lyot filter, the PMF works as the birefringent element, and the input fiber polarizer and output fiber polarizer play the roles of a polarizer and a polarization analyzer, respectively. From Fig. 1, we can clearly see that the incident light will transmit through the input fiber polarizer, the PMF and the output fiber polarizer in sequential order. As a polarizer, the input fiber polarizer will convert the input light into linearly polarized light. Then, the linearly polarized light will enter into the PMF. Due to the birefringence of the PMF, the linearly polarized light will be subsequently resolved into two paths that travel along the fast-axis and slow-axis at different phase velocities. In the output fiber polarizer, the two beams with a phase difference will be combined, resulting in interference of linear polarization status.

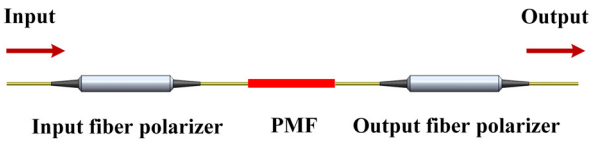

FIGURE 1. Schematic diagram of the proposed all-fiber Lyot filter consisting of a PMF cavity sandwiched by two linear fiber polarizers.

For the Lyot filter, the normalized transmittance T can be given by [36]

$$T = \sin^2\alpha \sin^2\beta + \cos^2\alpha \cos^2\beta + \frac{1}{2}\sin 2\alpha \sin 2\beta \cos\Delta\varphi \tag{1}$$

Here, α, β are the angles between the linear polarization directions of the two fiber polarizers and the direction of the slow-axis in the PMF, respectively. $\Delta\varphi$ is defined as the phase difference induced by the PMF based birefringence cavity, which can be given by the equation as follows:

$$\Delta\varphi = \frac{2\pi L_{HB-SMF}\Delta n}{\lambda} \tag{2}$$

where L_{PMF} is the length of the PMF based birefringence cavity, Δn is the birefringence of the employed PMF and λ is the working wavelength of the incident light. From Eq. (1) and (2), we can find that the normalized transmittance T is a cosine function of the working wavelength λ. When the phase difference $\Delta\varphi$ satisfies the condition of $\Delta\varphi = (2m+1)\pi$ (m is a nonnegative integer), the normalized transmittance T attains the minimum value, corresponding to the dip in the transmission spectrum. The corresponding wavelength of the dip can be expressed as:

$$\lambda_{dip} = \frac{2L_{PMF}\Delta n}{2m+1} \tag{3}$$

Accordingly, the free spectrum range (FSR), namely the wavelength interval of the adjacent dips, can be given by:

$$FSR_{Lyot} = \frac{\lambda_{dip}^2}{L_{PMF}\Delta n} \tag{4}$$

According to Eq. (1)-(4), it can be concluded that in the interference spectrum of Lyot filter, the fringe visibility is only related to the angles of α and β, and the wavelength λ_{dip} of the dip and the FSR are associated only with the length L_{PMF} and the birefringence Δn of the employed PMF. In the proposed Lyot filter, the employed PMF is the Panda fiber, which is a common birefringence fiber that has a high thermal optical coefficient. When there is a variation in temperature, the thermo-optic effect will bring about a variation in the birefringence Δn, and the dip wavelength λ_{dip} will correspondingly have a shift. This provides a mechanism to achieve the temperature sensing with the Lyot filter by tracking the shift of the dip wavelength in the interference spectrum.

To confirm the feasibility of the above mentioned mechanism for temperature sensing, the temperature test on the Lyot filter is conducted with the experiment setup shown in Fig. 2(a). In the experiment, a broadband light source (BBS, YSL Photonics SC-5) with the working wavelength ranging from 1000 nm to 1700 nm is employed as the input light source. At the same time, a commercial optical spectrum analyzer (OSA, Yokogawa AQ6370C) with an operation wavelength ranges from 600 nm to 1700 nm is used to record the output spectrum of Lyot filter. To track the evolution of interference spectrum in real-time under

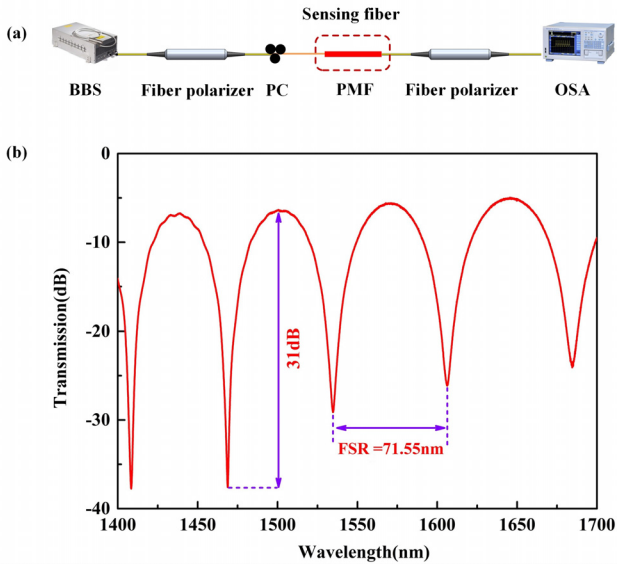

FIGURE 2. (a) Experiment setup for temperature sensing with Lyot filter based temperature sensor. (b) The output spectrum of the Lyot filter under room temperature.

different temperature, the input end and output end of the Lyot filter are directly connected to the BBS and the OSA, respectively. The Lyot filter is simple comprised of a 9.5 cm long PMF based birefringence cavity positioned between two parallel linear fiber polarizers. The employ PMF is a commercial PMF (PM-1550, YOFC), which has a birefringence of 2.28×10^{-4}. In addition, as the fringe visibility of the interference spectrum is depend on the angles of α and β, a polarization controller (PC) is inserted between the input fiber polarizer and the PMF to adjust the angle α to get a desired fringe visibility. And yet, the PC is not essential in the practical application as the angle α and β can be precisely pre-set with a Polarization Maintaining Fiber Fusion Splicer (FSM-100P+, FUJIKURA). Figure 2(b) is the obtained output spectrum of the Lyot filter under room temperature in the wavelength ranging from 1400 nm to 1700 nm. From Fig. 2(b), it can be clearly seen that the output spectrum of the Lyot filter is a typically interference spectrum that the intensity changes periodically with the wavelength. The FSR of the interference spectrum around 1550 nm is 71.55 nm, corresponding to the 9.5 cm long PMF based birefringence cavity. In addition, the obtained maximal fringe visibility is up to ~31 dB around 1550 nm, which is well suited to the requirements of the wavelength interrogation technique used for this sensor.

To experimentally investigate the temperature characteristic of Lyot filter, the PMF as the sensor head is heated by a temperature-controlled furnace from 25 °C to 50 °C with an increment of 5 °C, and the corresponding interference spectra of the Lyot filter under different temperatures are recorded by the OSA with a resolution of 0.5 nm in real-time. Figure 3(a) is the recorded interference spectrum evolution of the Lyot filter in the wavelength from 1475 nm to 1625 nm under each temperature. One can clearly see from Fig. 3(a) that

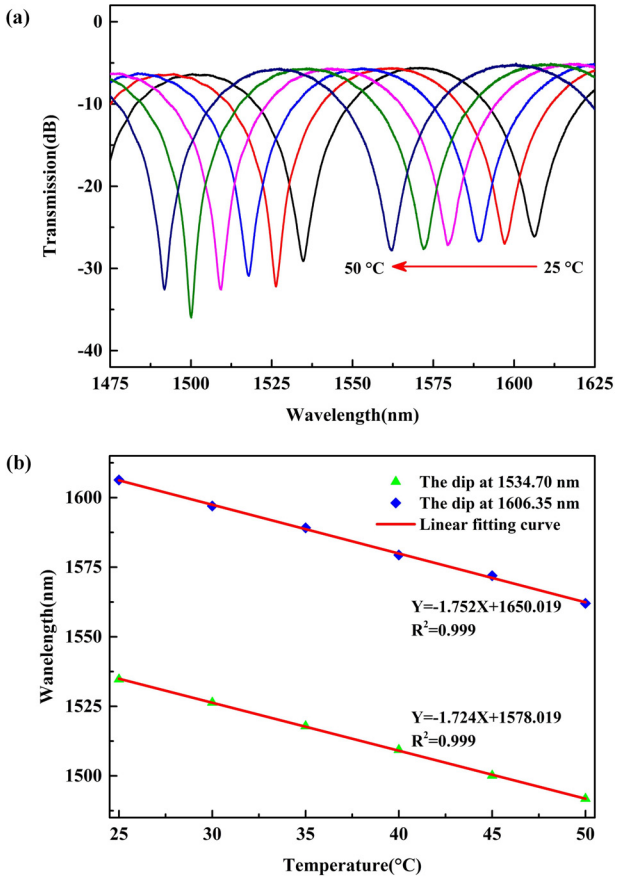

FIGURE 3. (a) Recorded interference spectrum evolution of the Lyot filter under the temperature from 25 °C to 50 °C. (b) Relationship between the selected dip wavelengths and temperature.

with the increase of temperature, the wavelength of the dip shifts to the shorter wavelength, namely blue shift. Under the temperature variation of 25 °C, the temperature-induced wavelength shifts of the dip at 1534.70 nm and 1606.35 nm are 42.90 nm and 44.35 nm, respectively. Figure 4(b) depicts the relationship between the selected two dip wavelengths and temperature. By linear fitting, one can observe that the selected two dip wavelengths change linearly with the temperature, confirming the feasibility of Lyot filter based temperature sensor. The slopes of the obtained two linear fitting curves are -1.724 and -1.752, corresponding to the temperature sensitivities of -1.724 nm/°C and -1.752 nm/°C, respectively.

For the Lyot filter based temperature sensor, the temperature sensitivity S_T at the selected dip wavelength λ_{dip} can be derived from Eq. (3) as [41]:

$$S_T = \frac{d\lambda_{dip}}{dT} = \frac{\lambda_{dip}}{L}\frac{\partial L}{\partial T} + \frac{\lambda_{dip}}{\Delta n}\frac{\partial \Delta n}{\partial T} = \lambda_{dip}K_\alpha + \frac{\lambda_{dip}}{\Delta n}K_T \tag{5}$$

Here, K_α and K_T are the thermal expansion coefficient and thermo-optical coefficient of the employed PMF, respectively. In view of that thermal expansion coefficient K_α of silica type fiber is 5×10^{-7} /°C, the contribution from thermal expansion effect to the temperature sensitivity S_T is so small that can be neglected. Thus, the temperature sensitivity S_T of the Lyot filter based temperature sensor can be simplified as:

$$S_T = \frac{\lambda_{dip}}{\Delta n}K_T \tag{6}$$

From Eq. (6), it can be concluded that the temperature sensitivity S_T is only rest with the thermo-optical coefficient of the employed PMF. The thermo-optical coefficient is a parameter of the PMF itself-inherent, which means that the temperature sensitivity S_T is a constant as long as the PMF employed in the Lyot filter is selected. In the practical application, by employing a PMF with a higher therm-optical coefficient, the achieved temperature sensitivity of the proposed Lyot filter based temperature sensor can be further improved.

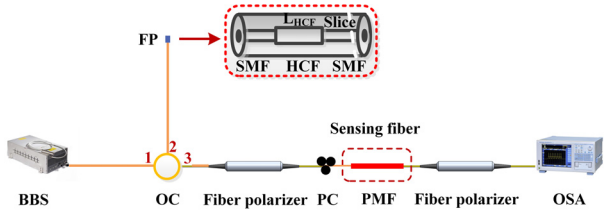

FIGURE 4. Configuration of the temperature sensing system based on Lyot filter with Vernier effect.

III. TEMPERATURE CHARACTERISTIC OF LYOT FILTER WITH VERNIER EFFECT

Instead of employing a PMF with a higher thermo-optical coefficient, the sensitivity of the proposed Lyot filter based temperature sensor is improved by introduced Vernier effect. Figure 4 illustrates the configuration of the temperature sensing system based on Lyot filter with Vernier effect. In the temperature sensing system, Vernier effect is introduced by cascading a FPI with the Lyot filter. The employed FPI is comprised of a hollow core fiber (HCF) sandwiched by single mode fiber (SMF). The inner diameter and outer diameter of the employed HCF are 10 μm and 125 μm, respectively. To eliminate the parasitic interference generated from the end facet reflection, the output end of the FPI is sliced with a tilt angle. The BBS, FPI and Lyot filter are connected to the ports 1, 2, and 3 of an optical circulator (OC), respectively. The OSA is connected to the output end of the Lyot filter. Thus, the superimposed spectrum of the cascaded FPI and Lyot filter can be observed by the OSA. In addition, to observe an obviously Vernier effect in the superimposed spectrum, the FSRs of the two interferometers must be close but not equal, which could be achieved by accurately controlling the length of the employed HCF in the experiment.

Figure 5(a) is the measured interference spectra of FP and Lyot filter under room temperature, respectively. For the Lyot filter, the length of the employed PMF is 65 cm, corresponding to the FSR_s of 10.10 nm in the interference spectrum. To get an FSR_r that close to FSR_s, the length of the employed HCF is accurately controlled by a homemade microscope-assisted fiber cutter, and the final obtained FSR_r

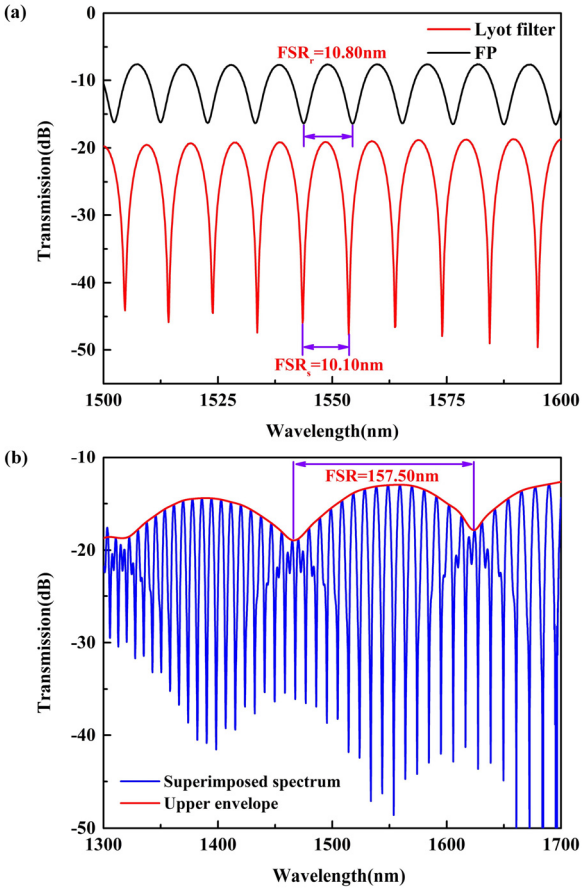

FIGURE 5. (a) Interference spectra of FP and Lyot filter. (b) Superimposed spectrum of the cascaded FPI and Lyot filter.

is 10.80 nm. Figure 5(b) is the superimposed spectrum of the cascaded FPI and Lyot filter, which consists of a series of fringes with different amplitude, confirming the generation of Vernier effect. Although the employed PM fiber, optical circulator, and polarizer all have bandwidths, the obtained superimposed spectrum shows that the proposed sensor can be work in the wavelength ranging from 1300 nm to 1700 nm, which means that the bandwidth of the above devices will not influence the sensor's performance. By using curve fitting method, the upper envelope profile of superimposed spectrum is extracted and shown in Fig. 5(b) with the red curve. The measured FSR of the upper envelope is ∼157.50 nm.

According to the theory of Vernier effect, the FSR of the upper envelope can be given by [42]:

$$FSR_{Upper} = \frac{FSR_r \cdot FSR_s}{|FSR_r - FSR_s|} \tag{7}$$

Here, FSR_r and FSR_s are the FSRs of the reference interferometer and sensing interferometer, respectively. From Eq. (7), we can know that, to get a desired FSR_{Upper}, the PMF employed in the Lyot filter and the HCF employed in the FPI should have the appropriate length, respectively. In our experiment, the FPI and Lyot filter work as the reference interferometer and sensing interferometer, respectively, and the corresponding FSR_r and FSR_s are 10.80 nm and 10.10 nm.

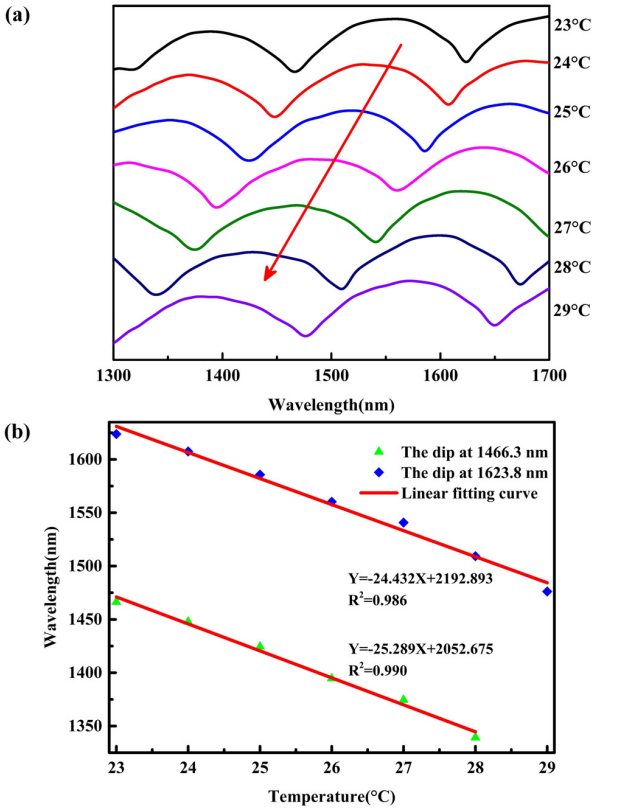

FIGURE 6. (a) Recorded spectrum evolution of the upper envelope under the temperature from 23 °C to 29 °C. (b) Relationship between the selected dip wavelengths of the upper envelope and temperature.

According to Eq. (7), the theoretical calculated value of the FSR is 156.83 nm, which is consistent with the experiment result.

The experiment to investigate the temperature characteristic of Lyot filter with Vernier effect is carried out with the experiment setup shown in Fig. 4. In the experiment, the PMF in Lyot filter is employed as the sensing fiber and heated from 23 °C to 29 °C, and the corresponding interference spectra are recorded in real time by the OSA. Figure 6(a) illustrates the obtained spectrum evolution of the upper envelope under different temperatures. Similar to the temperature response of Lyot filter, there is a blue shift in the upper envelope. And yet, the difference is mainly in the amount wavelength shift induced by the temperature variation. Compared with the wavelength shift of 44.35 nm under the temperature variation of 25 °C in the Lyot filter, the wavelength shift of the upper envelope is up to 147.60 nm under the temperature variation of 6 °C. Furthermore, the relationship between the selected dip wavelengths of the upper envelope and temperature is presented in Fig. 6(b). One can clearly see that there is a linear relationship between the selected dip wavelengths and temperature. For the selected dip wavelengths at 1466.3 nm and 1623.8 nm, the wavelength-temperature coefficient are −25.289 and −24.432, corresponding to the temperature sensitivities of −25.289 nm/°C and −24.432 nm/°C, respectively. In comparison with the temperature sensitivity of Lyot filter, the temperature sensitivity can be magnified

about 15 times. Although the achieved temperature sensitivity is significantly high, the structure of the proposed temperature sensor is relatively complex. To further simplify the structure, the proposed temperature sensor can be achieved by cascading a FPI with a reflective Lyot filter. And the reflective Lyot filter is only consist of a single 45°-tilted fiber gratings based fiber polarizer and a segment of femtosecond laser-induced high birefringence single-mode fiber. In this way, the structure of the proposed temperature sensor can be simplified and work in reflection mode.

For the Lyot filter with Vernier effect, the improved temperature sensitivity S can be expressed as [42]:

$$S = M \cdot S_T \tag{8}$$

where M is the amplification factor referring to Vernier effect, which can be given by [42]:

$$M = \frac{FSR_r}{|FSR_r - FSR_s|} \tag{9}$$

In view of that the values of FSR_r and FSR_s are 10.80 nm and 10.10 nm, the theoretical calculated amplification factor M is about 15. The theoretical analysis agrees well with the experiment result, confirming the feasibility of highly sensitive temperature sensor based on all-fiber polarization interference filter with Vernier effect. In addition, according to Eq. (8) and (9), it can be concluded that the achieved temperature sensitivity S can be further improved by accurately controlling the lengths of the PMF employed in Lyot filter and the HCF employed in the FPI.

IV. CONCLUSION

In conclusion, a novel highly sensitive temperature sensor based on all-fiber polarization interference filter with Vernier effect is proposed and experimentally demonstrated in this article. The all-fiber polarization interference filter employed in the experiment is Lyot filter, which is simply comprised of a PMF based birefringence cavity sandwiched by two linear fiber polarizers. Experimental results show that a single Lyot filter can achieve temperature sensing with a sensitivity of −1.752 nm/°C, confirming the feasibility of Lyot filter based temperature sensor. To further improve the temperature sensitivity, Vernier effect is introduced into the Lyot filter by simply cascading a Fabry–Perot interference. With the help of Vernier effect, the temperature sensitivity of the Lyot filter is improved to −25.289 nm/°C, indicating the good performance of Lyot filter with Vernier effect in temperature sensing. With the high sensitivity, simple structure and all-fiber configuration, the proposed sensor is highly desirable for temperature sensing.

REFERENCES

[1] B. Huang and X. Shu, "Ultra-compact strain-and temperature-insensitive torsion sensor based on a line-by-line inscribed phase-shifted FBG," *Opt. Express*, vol. 24, no. 16, pp. 17670–17679, 2016.
[2] B. Huang and X. Shu, "Highly sensitive torsion sensor with femtosecond laser-induced low birefringence single-mode fiber based Sagnac interferometer," *Opt. Express*, vol. 26, no. 4, pp. 4563–4571, Feb. 2018.
[3] B. Huang, X. Shu, Y. Wang, C. Mao, and Y. Wang, "Temperature-and strain-insensitive transverse load sensing based on optical fiber reflective Lyot filter," *Appl. Phys. Express*, vol. 12, no. 7, Jul. 2019, Art. no. 076501.
[4] S. Zhou, B. Huang, and X. Shu, "A multi-core fiber based interferometer for high temperature sensing," *Meas. Sci. Technol.*, vol. 28, no. 4, Apr. 2017, Art. no. 045107.
[5] B. Huang, Y. Wang, and C. Mao, "Temperature-independent gas pressure sensor with high birefringence photonic crystal fiber-based reflective Lyot filter," *Sensors*, vol. 19, no. 23, p. 5312, Dec. 2019.
[6] V. Bhatia, D. Campbell, R. O. Claus, and A. M. Vengsarkar, "Simultaneous strain and temperature measurement with long-period gratings," *Opt. Lett.*, vol. 22, no. 9, pp. 648–650, 1997.
[7] C. C. Ye, S. W. James, and R. P. Tatam, "Simultaneous temperature and bend sensing with long-period fiber gratings," *Opt. Lett.*, vol. 25, no. 14, pp. 1007–1009, Jul. 2000.
[8] Y. J. Rao, Y. P. Wang, Z. L. Ran, and T. Zhu, "Novel fiber-optic sensors based on long-period fiber gratings written by high-frequency CO_2 laser pulses," *J. Lightw. Technol.*, vol. 21, no. 5, pp. 1320–1327, 2003.
[9] A. P. Zhang, L.-Y. Shao, J.-F. Ding, and S. He, "Sandwiched long-period gratings for simultaneous measurement of refractive index and temperature," *IEEE Photon. Technol. Lett.*, vol. 17, no. 11, pp. 2397–2399, Nov. 2005.
[10] Y. Wang, W. Jin, and D. N. Wang, "Unique temperature sensing characteristics of CO_2-laser-notched long-period fiber gratings," *Opt. Lasers Eng.*, vol. 47, no. 10, pp. 1044–1048, Oct. 2009.
[11] D. Grobnic, S. J. Mihailov, C. W. Smelser, and H. Ding, "Sapphire fiber Bragg grating sensor made using femtosecond laser radiation for ultrahigh temperature applications," *IEEE Photon. Technol. Lett.*, vol. 16, no. 11, pp. 2505–2507, Nov. 2004.
[12] B. Zhang and M. Kahrizi, "High-temperature resistance fiber Bragg grating temperature sensor fabrication," *IEEE Sensors J.*, vol. 7, no. 4, pp. 586–591, Apr. 2007.
[13] S. Sengupta, S. K. Ghorai, and P. Biswas, "Design of superstructure fiber Bragg grating with efficient mode coupling for simultaneous strain and temperature measurement with low cross-sensitivity," *IEEE Sensors J.*, vol. 16, no. 22, pp. 7941–7949, Nov. 2016.
[14] S. Sridhar, S. Sebastian, and S. Asokan, "Temperature sensor based on multi-layer MoS_2 coated etched fiber Bragg grating," *Appl. Opt.*, vol. 58, no. 3, pp. 535–539, 2019.
[15] W.-H. Tsai and C.-J. Lin, "A novel structure for the intrinsic Fabry–Perot fiber-optic temperature sensor," *J. Lightw. Technol.*, vol. 19, no. 5, pp. 682–686, May 2001.
[16] J. Mathew, O. Schneller, D. Polyzos, D. Havermann, R. M. Carter, W. N. MacPherson, D. P. Hand, and R. R. J. Maier, "In-fiber Fabry–Perot cavity sensor for high-temperature applications," *J. Lightw. Technol.*, vol. 33, no. 12, pp. 2419–2425, 2015.
[17] Y. Zhang, L. Yuan, X. Lan, A. Kaur, J. Huang, and H. Xiao, "High-temperature fiber-optic Fabry–Perot interferometric pressure sensor fabricated by femtosecond laser," *Opt. Lett.*, vol. 38, no. 22, pp. 4609–4612, 2013.
[18] C. Zhu, Y. Zhuang, B. Zhang, M. Roman, P. Wang, and J. Huang, "A miniaturized optical fiber tip high-temperature sensor based on concave-shaped Fabry–Perot cavity," *IEEE Photon. Technol. Lett.*, vol. 31, no. 1, pp. 35–38, Jan. 1, 2019.
[19] L. Yuan, T. Wei, Q. Han, H. Z. Wang, J. Huang, L. Jiang, and H. Xiao, "Fiber inline Michelson interferometer fabricated by a femtosecond laser," *Opt. Lett.*, vol. 37, no. 21, pp. 4489–4491, Nov. 2012.
[20] J. Yin, T. Liu, J. Jiang, K. Liu, S. Wang, S. Zou, and F. Wu, "Assembly-free-based fiber-optic micro-michelson interferometer for high temperature sensing," *IEEE Photon. Technol. Lett.*, vol. 28, no. 6, pp. 625–628, Mar. 15, 2016.
[21] Y. Wang, Y. Li, C. Liao, D. N. Wang, M. Yang, and P. Lu, "High-temperature sensing using miniaturized fiber in-line Mach–Zehnder interferometer," *IEEE Photon. Technol. Lett.*, vol. 22, no. 1, pp. 39–41, 2010.
[22] L. Jiang, J. Yang, S. Wang, B. Li, and M. Wang, "Fiber Mach–Zehnder interferometer based on microcavities for high-temperature sensing with high sensitivity," *Opt. Lett.*, vol. 36, no. 9, pp. 3753–3755, 2011.
[23] A. A. Jasim, S. W. Harun, H. Arof, and H. Ahmad, "Inline microfiber Mach–Zehnder interferometer for high temperature sensing," *IEEE Sensors J.*, vol. 13, no. 2, pp. 626–628, Feb. 2013.
[24] A. N. Starodumov, L. A. Zenteno, D. Monzon, and E. De La Rosa, "Fiber Sagnac interferometer temperature sensor," *Appl. Phys. Lett.*, vol. 70, no. 1, pp. 19–21, Jan. 1997.

[25] D. S. Moon, B. H. Kim, A. Lin, G. Sun, Y. G. Han, W.-T. Han, and Y. Chung, "The temperature sensitivity of Sagnac loop interferometer based on polarization maintaining side-hole fiber," *Opt. Express*, vol. 15, no. 13, pp. 7962–7967, Jun. 2007.
[26] J. Zhang, X. Qiao, T. Guo, Y. Weng, R. Wang, Y. Ma, Q. Rong, M. Hu, and Z. Feng, "Highly sensitive temperature sensor using PANDA fiber Sagnac interferometer," *J. Lightw. Technol.*, vol. 29, no. 24, pp. 3640–3644, Dec. 2011.
[27] Y. Cui, P. P. Shum, D. J. J. Hu, G. H. Wang, G. Humbert, and X. Q. Dinh, "Temperature sensor by using selectively filled photonic crystal fiber Sagnac interferometer," *IEEE Photon. J.*, vol. 4, no. 5, pp. 1801–1808, Oct. 2012.
[28] Y. Xin, X. Dong, Q. Meng, F. Qi, and C.-L. Zhao, "Alcohol-filled side-hole fiber Sagnac interferometer for temperature measurement," *Sens. Actuators A, Phys.*, vol. 193, pp. 182–185, Apr. 2013.
[29] E. Reyes-Vera, C. M. B. Cordeiro, and P. Torres, "Highly sensitive temperature sensor using a Sagnac loop interferometer based on a side-hole photonic crystal fiber filled with metal," *Appl. Opt.*, vol. 56, no. 2, pp. 156–162, 2017.
[30] W. Jin, X. Li, S. H. Wu, X. H. Fu, G. W. Fu, M. M. Bilal, and W. H. Bi, "Highly sensitive temperature sensing probes based on liquid cladding elliptical micro/nanofibers," *Opt. Express*, vol. 28, no. 14, pp. 20062–20073, 2020.
[31] B. Lyot, "Optical apparatus with wide field using interference of polarized light," *CR. Acad. Sci. (Paris)*, vol. 197, p. 1593, 1933.
[32] C.-Y. Chen, C.-L. Pan, C.-F. Hsieh, Y.-F. Lin, and R.-P. Pan, "Liquid-crystal-based terahertz tunable Lyot filter," *Appl. Phys. Lett.*, vol. 88, no. 10, Mar. 2006, Art. no. 101107.
[33] O. Aharon and I. Abdulhalim, "Liquid crystal Lyot tunable filter with extended free spectral range," *Opt. Express*, vol. 17, no. 14, pp. 11426–11433, 2009.
[34] A. Gorman, D. W. Fletcher-Holmes, and A. R. Harvey, "Generalization of the Lyot filter and its application to snapshot spectral imaging," *Opt. Express*, vol. 18, no. 6, pp. 5602–5608, 2010.
[35] C. O'Riordan, M. J. Connelly, P. M. Anandarajah, R. Maher, and L. P. Barry, "Lyot filter based multiwavelength fiber ring laser actively mode-locked at 10GHz using an electroabsorption modulator," *Opt. Commun.*, vol. 281, no. 13, pp. 3538–3541, Jul. 2008.
[36] K. E. Zoiros, C. O'Riordan, and M. J. Connelly, "Semiconductor optical amplifier pattern effect suppression using Lyot filter," *Electron. Lett.*, vol. 45, no. 23, pp. 1187–1189, Nov. 2009.
[37] Z. Yan, C. Mou, H. Wang, K. Zhou, Y. Wang, W. Zhao, and L. Zhang, "All-fiber polarization interference filters based on 45°-tilted fiber gratings," *Opt. Lett.*, vol. 37, no. 3, pp. 353–355, 2012.
[38] Z. Yan, H. Wang, K. Zhou, Y. Wang, W. Zhao, and L. Zhang, "Broadband tunable all-fiber polarization interference filter based on 45° tilted fiber gratings," *J. Lightw. Technol.*, vol. 31, no. 1, pp. 94–98, Jan. 1, 2013.
[39] B. Huang and X. Shu, "Highly sensitive twist sensor based on temperature- and strain-independent fiber lyot filter," *J. Lightw. Technol.*, vol. 35, no. 10, pp. 2026–2031, May 15, 2017.
[40] B. Huang, X. W. Shu, and Y. Q. Du, "Intensity modulated torsion sensor based on optical fiber reflective Lyot filter," *Opt. Express*, vol. 25, no. 5, pp. 5081–5090, 2017.
[41] B. Huang, Y. Wang, and C. Mao, "Lyot filter with femtosecond laser-induced high birefringence single-mode fiber for torsion, transverse load and temperature sensing," *IEEE Access*, vol. 8, pp. 25764–25769, 2020.
[42] Z. Xu, X. Shu, and H. Fu, "Sensitivity enhanced fiber sensor based on a fiber ring microwave photonic filter with the Vernier effect," *Opt. Express*, vol. 25, no. 18, pp. 21559–21566, Sep. 2017.

BO HUANG was born in Hubei, China, in 1990. He received the Ph.D. degree from the Wuhan National Laboratory for Optoelectronics, Huazhong University of Science and Technology, Wuhan, in 2018. Since 2018, he has been a Postdoctoral Research Fellow with the Key Laboratory of Optoelectronic Devices and Systems, Ministry of Education and Guangdong Province, College of Physics and Optoelectronic Engineering, Shenzhen University, Shenzhen, China. His current research interests include femtosecond laser micromachining and optical fiber sensors.

YING WANG was born in Henan, China, in 1983. He received the B.S. degree in applied physics and the Ph.D. degree in physical electronics from the Huazhong University of Science and Technology, Wuhan, China, in 2004 and 2010, respectively. From 2010 to 2015, he was a Research Associate with the Department of Electrical Engineering, The Hong Kong Polytechnic University, Hong Kong. Since 2015, he has been an Associate Professor with the College of Physics and Optoelectronic Engineering, Shenzhen University, Shenzhen, China. His research interests include optical fiber sensors and femtosecond laser micromachining.

CHANGRUI LIAO (Member, IEEE) was born in Shandong, China, in 1984. He received the B.Eng. degree in optical engineering and the M.S. degree in physical electronics from the Huazhong University of Science and Technology, Wuhan, China, in 2005 and 2007, respectively, and the Ph.D. degree in electrical engineering from The Hong Kong Polytechnic University, Hong Kong, in 2012. He is currently an Associate Professor with Shenzhen University, Shenzhen, China. His current research interests include femtosecond laser micromachining, optical fiber sensors, and optical microfluidics.

YIPING WANG (Senior Member, IEEE) was born in Chongqing, China, in 1971. He received the B.Eng. degree in precision instrument engineering from the Xi'an Institute of Technology, Xi'an, China, in 1995, and the M.S. and Ph.D. degrees in optical engineering from Chongqing University, Chongqing, China, in 2000 and 2003, respectively. From 2003 to 2005, he was a Postdoctoral Fellow with Shanghai Jiao Tong University, China. From 2005 to 2007, he was a Postdoctoral Fellow with The Hong Kong Polytechnic University. From 2007 to 2009, he was a Humboldt Research Fellow with the Institute of Photonic Technology, Jena, Germany. From 2009 to 2011, he was a Marie Curie Fellow with the Optoelectronics Research Centre, University of Southampton, U.K. Since 2012, he has been a Distinguished Professor with Shenzhen University, Shenzhen, China. He has authored or coauthored one book, 21 patent applications, and more than 240 journal and conference papers. His current research interests include optical fiber sensors, fiber gratings, and photonic crystal fibers.

Dr. Wang is a Senior Member of the Optical Society of America and of the Chinese Optical Society.